

# Scintillation Products Technical Note

Lanthanum Bromide Scintillators  
Performance Summary  
(Revision: June 2021)

## INTRODUCTION –

Since the discovery of  $\text{LaBr}_3:\text{Ce}$  as scintillators by Delft and Bern Universities<sup>1,2</sup>, several groups have furthered understanding of their properties; and Saint-Gobain Crystals has made considerable progress in their commercial availability.

In this summary, we report the performance of  $\text{LaBr}_3:\text{Ce}$  detectors and extend results to the 3” diameter, 3” long (“3x3”) crystals, drawing mainly from results published or presented elsewhere<sup>3,4,5</sup>. We are not attempting a comprehensive review and remind the reader that a partial compilation of the general literature is available on our website, [www.crystals.saint-gobain.com](http://www.crystals.saint-gobain.com). A table of scintillator properties is found at the end of this summary, we note in particular that  $\text{LaBr}_3:\text{Ce}$  crystals emit some 60% more light than  $\text{NaI}(\text{TI})$  for energies near 1 MeV and have much faster decay times and better timing properties.

Herein we cover energy resolution and relative efficiency as a function of gamma-ray energy emphasizing a comparison of  $\text{LaBr}_3:\text{Ce}$  and  $\text{NaI}(\text{TI})$  detectors for the 3”x3” size. We also take a look at performance versus temperature, performance versus count rate, coincidence resolving time, and intrinsic background.

## PERFORMANCE -

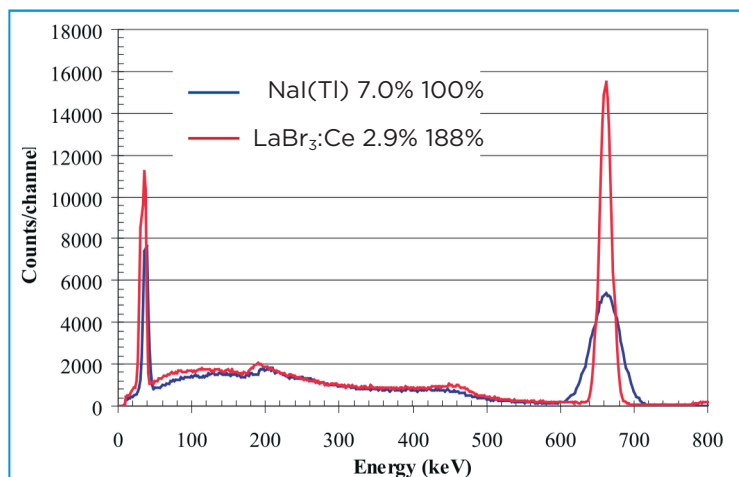
### Energy Resolution versus Energy

The energy resolution for  $\text{LaBr}_3\text{:Ce}$  crystals is determined both by their high light output and by their excellent energy linearity.

For the results reported in this subsection, 3" diameter, 3" long  $\text{LaBr}_3\text{:Ce}$  and  $\text{NaI(Tl)}$  detectors were compared. They were both in integrated packages, i.e., coupled directly to a 3" diameter photomultiplier - a Photonis XP5300B for the  $\text{LaBr}_3\text{:Ce}$  detector and an ETI 9305 for the  $\text{NaI(Tl)}$ . The source was "end-on", i.e., on axis with the detector. When the source was changed from one isotope to another, the distance was adjusted to achieve reasonable counting rates of a few thousand per second, and that same distance was used for both detectors so that efficiencies could be compared directly.

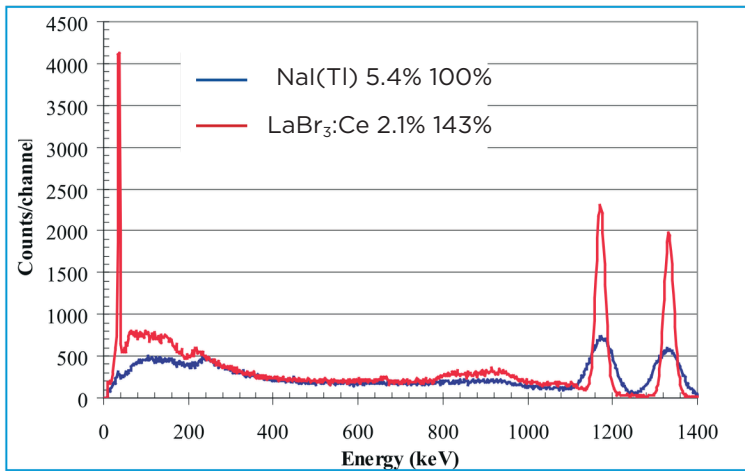
We begin the comparison with the response of the two detectors to  $^{137}\text{Cs}$  (662keV) and Figure 1, where the 3"x3" detector spectra are compared. Both the source's gamma ray at 662 keV and its barium Ka X-ray at 32 keV are shown. Spectra are normalized to 662 keV on the energy scale.

The figure also reports the areas under the 662 keV photopeak, set as 100% for  $\text{NaI(Tl)}$  and giving 118% as the relative efficiency for the  $\text{LaBr}_3\text{:Ce}$  unit primarily due to its higher density. For  $\text{NaI(Tl)}$  the peak near 32 keV is slightly higher on the energy scale than the one for the BrillLanCe 380 detector because  $\text{NaI(Tl)}$  is non-linear, producing a bit more light per keV at lower energies than at higher ones.



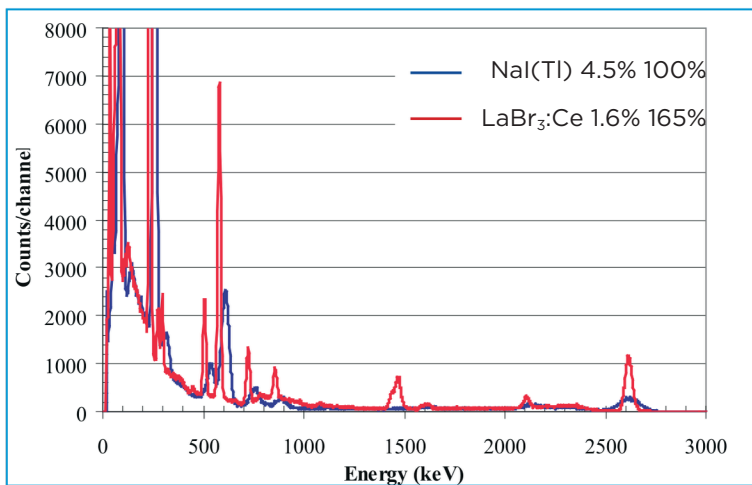
*Figure 1*  
Comparison of 3"x3" spectra for  $^{137}\text{Cs}$  (662 keV)  
 $\text{LaBr}_3\text{:Ce}$  detector (red) and  $\text{NaI(Tl)}$  (blue)

Figure 2 shows the response of the two detectors for  $^{60}\text{Co}$  where the well-known lines at 1332 and 1173 keV are seen. At 1332 keV, the BrillLanCe 380 unit gives 2.1% energy resolution versus 5.4% for the NaI(Tl) unit. The BrillLanCe 380 detector is 43% more efficient. In addition, a line is seen in the 35 keV region in the BrillLanCe 380 curve. This is due to emission of Ba X-rays from  $^{138}\text{La}$  background which is discussed in detail below.



*Figure 2*  
Comparison of 3"x3" spectra for  $^{60}\text{Co}$   
LaBr<sub>3</sub>:Ce detector (red) and NaI(Tl) (blue)

At 2615 keV ( $^{208}\text{Tl}$  in the thorium decay chain), the LaBr<sub>3</sub>:Ce detector achieves 1.6% energy resolution versus NaI(Tl)'s 4.5% and is 65% more efficient as seen in Figure 3. Again, spectra are normalized at the highest energy line, 2615 keV, and energy offsets are seen between the two materials at lower energies due to the differences in linearity. The improvement in spectral resolution with the LaBr<sub>3</sub>:Ce package is particularly apparent in this multiple energy spectrum. The line seen just below 1500 keV in the LaBr<sub>3</sub>:Ce spectrum is again due to background and will be discussed further.



*Figure 3*  
Comparison of 3"x3" spectra for the Thorium  
decay chain.  
LaBr<sub>3</sub>:Ce detector (red) and NaI(Tl) (blue)

The advantages of BriLanCe 380 detectors continue to low energies as seen in Figure 4, which shows the response to  $^{57}\text{Co}$ . The BriLanCe 380 detector clearly resolves the 136 keV line from the 122 keV line while NaI(Tl) does not. The background from Ba X-ray lines in the 35 keV region is also seen in the BriLanCe 380 spectrum.

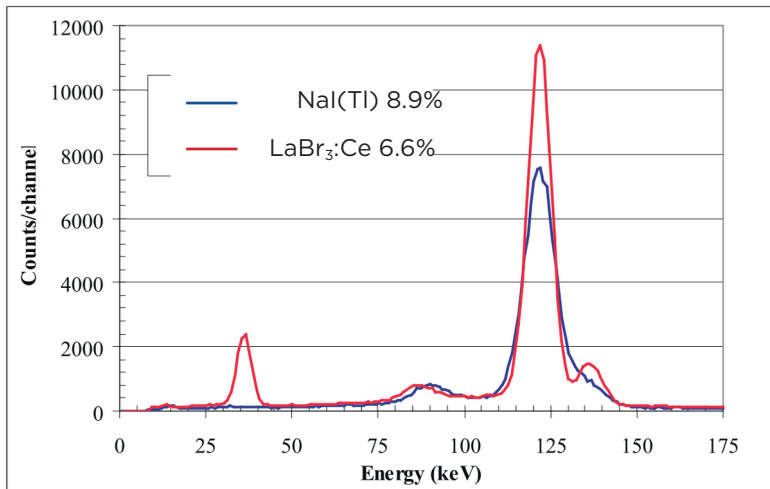


Figure 4  
Comparison of 3"x3" spectra for  $^{57}\text{Co}$   
LaBr<sub>3</sub>:Ce detector (red) and NaI(Tl)  
(blue)

To complete the survey, Figure 5 shows a  $^{133}\text{Ba}$  spectrum for the two detectors. The LaBr<sub>3</sub>:Ce detector shows substantially better separation of the lines near 350 keV. Both detectors show prominent lines just above 30 keV due to Cs K $\alpha$  X-rays emitted by the source.

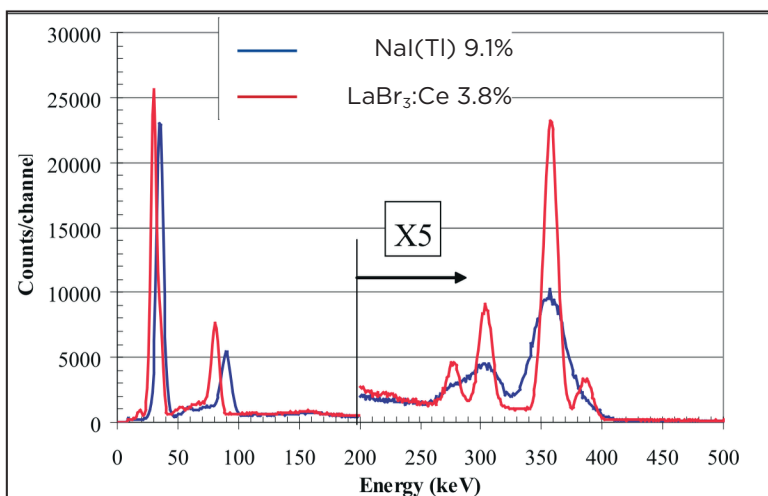


Figure 5  
Comparison of 3"x3" spectra for  $^{133}\text{Ba}$   
LaBr<sub>3</sub>:Ce detector (red) and NaI(Tl) (blue)

Table 1 summarizes the results from this section with energy resolution and relative efficiency tabulated for several of the energies presented. The advantages of BrillanCe 380 detectors over NaI(Tl) are seen at all energies.

Energy (keV)	Resolution LaBr <sub>3</sub> :Ce	Resolution NaI(Tl)	Ratio Peak Counts
356	6.6%	8.9%	1.05
662	3.8%	9.1%	1.06
1332	2.9%	7.0%	1.18
2615	2.1%	5.4%	1.43
422	1.6%	4.5%	1.65

Table 1 - Summary

3"x3" Detector Response vs. Energy Resolution and Relative Efficiency

The well-behaved nature of the energy resolution versus energy is displayed in Figure 6 with this data overlaid on points extracted from earlier work and smaller detectors. The energy resolution faithfully follows the square root of energy as expected statistically for linear detectors. Although it is not demonstrated, one can conclude from the data in Table 2 and Figure 6 that NaI(Tl) does not track this scheme.

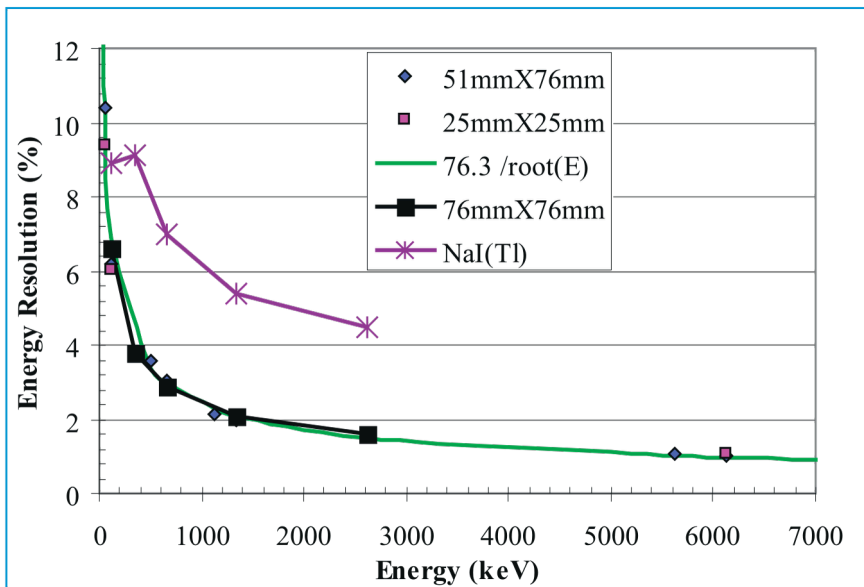


Figure 6  
Energy resolution as a function of energy

Cautionary Note

LaBr<sub>3</sub>:Ce scintillator has 1.6 times the light output and is more than 10 times faster than NaI(Tl). This can produce non-linear effects in the pmt. A simple calculation shows that the instantaneous charge pulse is about 25 times that of NaI(Tl). This is based on the ph ratio of 1.6 and multiplied by the faster time factor of 250ns/16ns specifically: 25X = 1.6X(250/16).

The non-linearity manifests itself in two ways. First, the FWHM of a peak is better than expected at that energy and second, the position of higher energy peaks will be at lesser pulse height than expected from a linear extrapolation. It is possible to verify that this is occurring by decreasing the HV by about 100V and observing an improvement in linearity and a correspondingly a slight decrease in FWHM. In order to keep these undesirable effects to a minimum, Saint-Gobain Crystals is selecting pmts that have superior linearity properties. Often these are 8-stage pmts.

Response versus Temperature

The remarkable properties of LaBr<sub>3</sub>:Ce crystals are preserved as temperature increases as shown in Figure 7, and light output is dramatically greater at high temperatures than it is for all other crystals tested. Recent testing confirms that LaBr<sub>3</sub>:Ce emits 160% of the light output of NaI(Tl) at room temperature in similar rugged, high temperature packages useful in oil well logging.

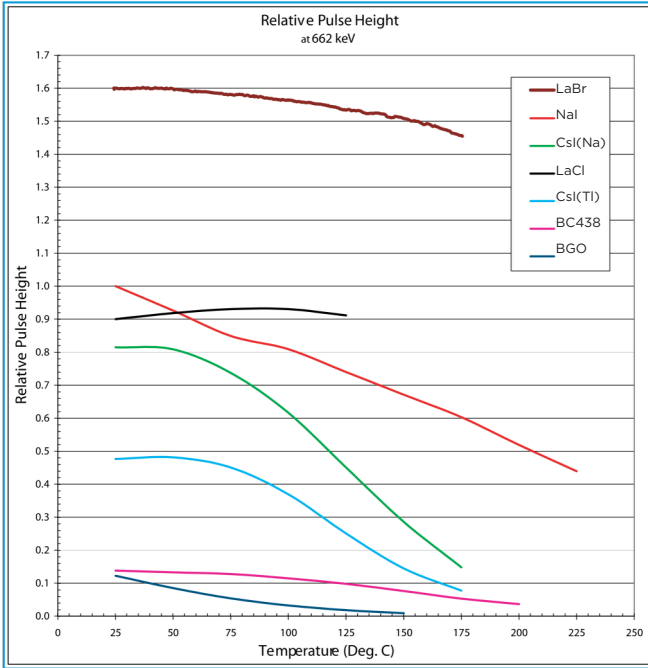


Figure 7  
Response of scintillator at temperature with Photomultiplier tube held at constant temperature.<sup>15</sup>

Response versus Rate

Given the ten-fold difference in decay time between NaI(Tl) and LaBr crystal, performance to high rate is expected and is displayed in Figure 8. These measurements used 1"x1" crystals and the same 8575 photomultiplier for each detector followed by a timing filter amplifier and constant fraction discriminator. Rate was adjusted by changing source strength and position.<sup>8</sup> This demonstration verifies the expected difference between materials, but detailed results are highly dependent on the electronics configuration chosen, of course.

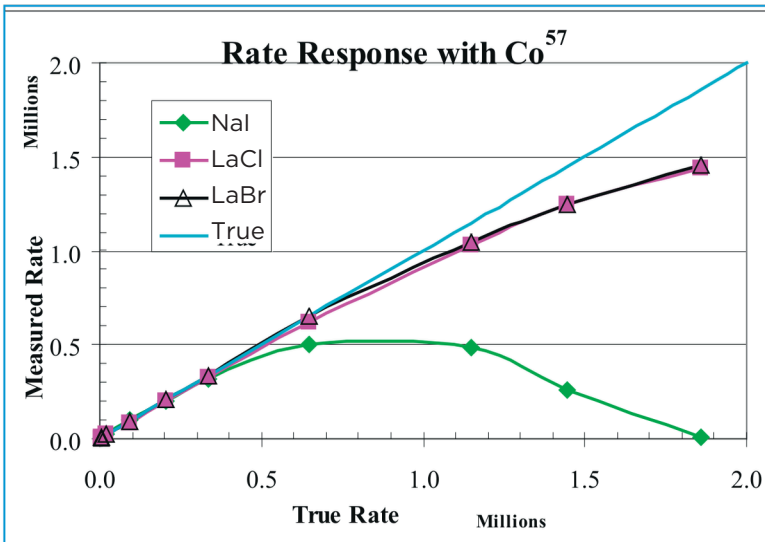


Figure 8  
Response versus Rate

## Coincidence Resolving Time

As expected from the decay time properties and high light output, the  $\text{LaBr}_3:\text{Ce}$  crystals have excellent timing properties. This is suggested by the figure of merit column in The Table of Scintillation Properties at the end of this summary. The figure of merit (F.O.M.) in column three is the square root of decay time divided by the light output and is an indication of the expected timing performance relative to other scintillators.  $\text{LaBr}_3:\text{Ce}$  crystals are fast enough that timing results also depend on light propagation times and thereby on crystal size (Figure 9). Other groups have shown that decay time is only a rudimentary indicator of rise time which is the more telling parameter, but more difficult to measure, and very dependent on the choice of photomultiplier.

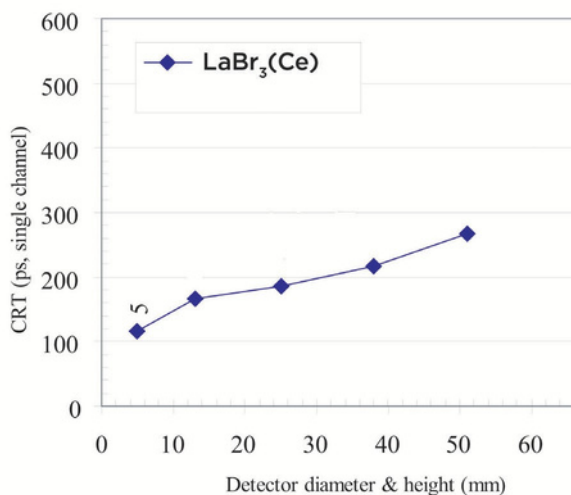
Representative coincidence resolving times (CRT) are shown in Figure 9a for various sizes of  $\text{LaBr}_3:\text{Ce}$  detectors. The data was taken using two Photonis XP20Y0 photomultipliers (PMTs). The PMT serving as the STOP channel was coupled to the crystal to be measured and the other PMT was coupled to a dedicated START crystal, a 4x4x5 mm  $\text{LaBr}_3:\text{Ce}$  crystal. This particular crystal had been previously measured with a “single channel” CRT value of 115 ps. “Single channel” value means the value that would be measured against an infinitely fast channel. CRT data were taken using a  $^{22}\text{Na}$  source. The system was gated such that only events which resulted in a 511 keV photopeak in both channels were counted.

Figure 9a shows that  $\text{LaBr}_3:\text{Ce}$  detectors have somewhat better CRT. We also see the dependence on crystal size, increasing as crystals and light transit times become larger. The 76 mm point is a special case because the Photonis XP20Y0 is a 51 mm diameter tube, and thus does not completely cover the crystal. When measuring this larger diameter crystal, a reflective annulus was placed to cover the area of the window which was not covered by the PMT. The effect of this geometry on CRT has not been quantified but probably increases its value.

Figure 9b shows the single channel CRT measured for a few geometries using a standard PMT with a plano-plano face plate. This is an important point because it is possible to maintain the excellent energy resolution of  $\text{LaBr}_3:\text{Ce}$  crystals with standard PMTs. Note that the CRT does depend critically on the PMT; for example, the XP2060 38mm PMT gives much poorer performance than the larger PMTs.

**Figure 9a**

Coincidence Resolving Time (CRT) of  $\text{LaBr}_3:\text{Ce}$  detectors as a function of the crystals' longest dimension measured with fast timing PMTs that have plano-concave face plates.



**Figure 9b**

Timing measured at 511keV with  $\text{LaBr}_3:\text{Ce}$  Integrated Detector

Size(mm)*	CRT** (ns)	PMT Size (mm)	PMT*** Type
25x25	1.08	38	XP2060
38x38	0.36	51	R6231
51x51	0.45	56	XP5500
76x76	0.49	76	XP5300

\* Diameter and length of right cylindrical crystal.

\*\* CRT is the Coincidence Resolving Time (single channel)

\*\*\* These are standard PMTs with plano-plano photocathode face plates.

### $^{138}\text{La}$ and $^{227}\text{Ac}$ Background

$^{138}\text{La}$  is a naturally occurring radioisotope of La with 0.09% abundance and has the decay scheme shown in Table 2.<sup>9</sup> In 66.4% of its decays,  $^{138}\text{La}$  undergoes electron capture (EC) to produce excited  $^{138}\text{Ba}$ , which in turn decays by emission of a 1436 keV gamma. A necessary byproduct of electron capture is refilling of the electron shell which results in emission of coincident barium X-rays in the 35 keV region. The remaining decays, 33.6%, proceed by beta emission to  $^{138}\text{Ce}$ , which decays by emitting a 789 keV gamma in coincidence with the beta having an end point energy of 255 keV.

The background spectrum is easily measured by self-counting. Figure 10 shows such a spectrum for a 1.5" x 1.5" detector (38x38 mm) counted for about 3 days (278278 sec) in a low background chamber. Reviewing the self-counting spectrum from left to right, we see first a beta continuum at low energies for  $^{138}\text{La}$  decays to  $^{138}\text{Ce}$  in which the 789 keV gamma has escaped the detector altogether. This beta-only spectrum continues to its end point of 255 keV. From about 255 to 750 keV the spectrum displays the Compton continua from the 789 and 1436 keV gamma rays. The 789 keV line is next as we proceed to higher energies, but since it is in coincidence with the beta, it is smeared to high energy in a gamma plus beta continuum ending a little above 1 MeV. Finally, we see the 1436 keV gamma, but displaced to a higher energy by approximately 37 keV to 1473 keV due to coincident capture of X-rays resulting when the Ba K level fills following K-electron capture. Similarly, the hump near 1441 keV on the low energy side of the 1473 line is due to the 1436 keV gamma plus 5 keV due to the 1436 keV gamma plus 5 keV due to coincident capture of X-rays when the Ba L-level fills following L-electron capture. The Ba K X-rays at 37 keV are only partially seen in Figure 10 due to the discriminator setting of the MCA. The sum line at 1473 keV might be used as a calibration peak, and while potentially interfering with detection of 40K at 1441 keV, has a constant and measurable activity that can be subtracted within statistical limits to determine 40K.

*Table 2*

*$^{138}\text{La}$  decay scheme.*

*(from 8th edition, Table of the Isotopes)<sup>9</sup>*

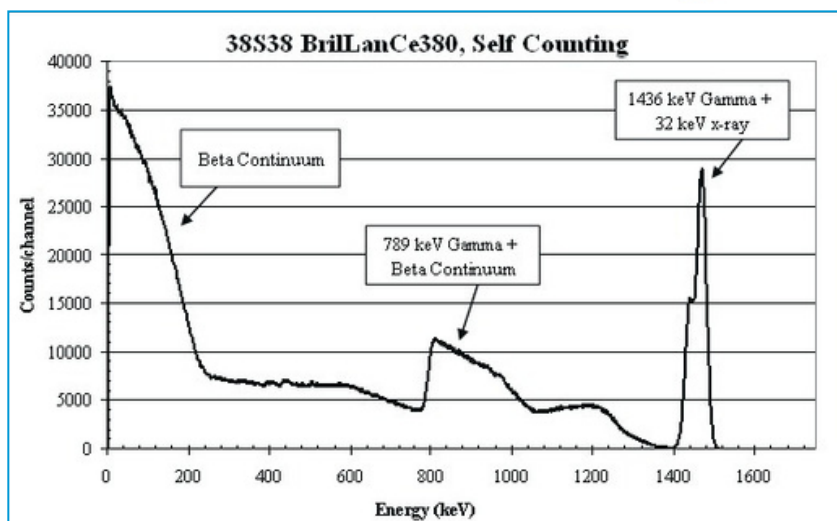
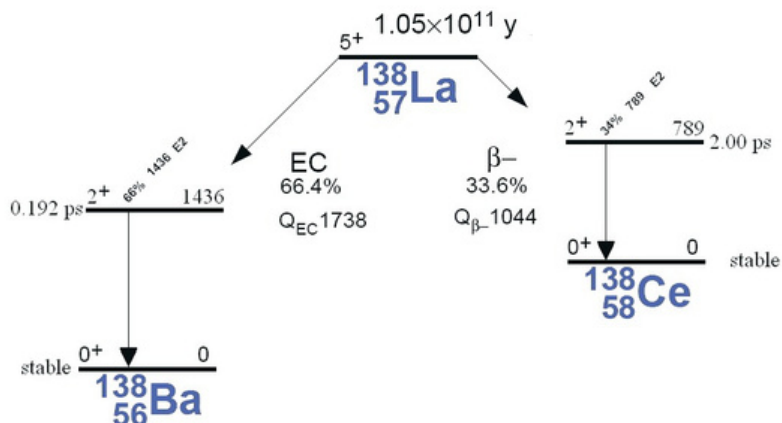
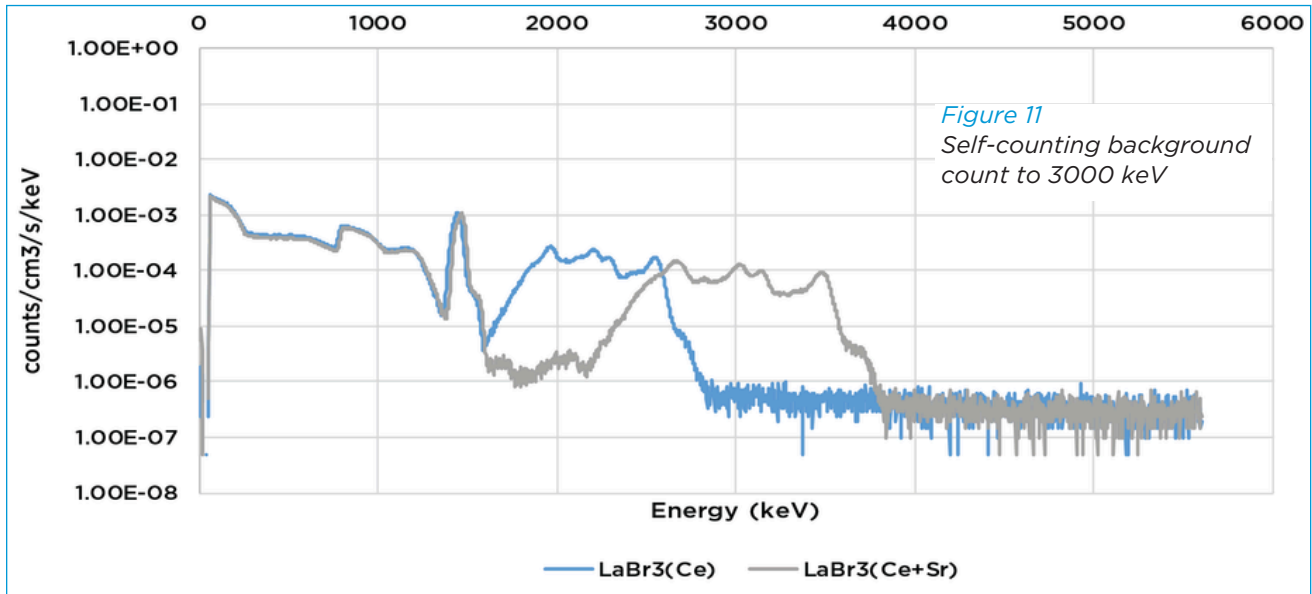


*Figure 10*

*Self-counting background spectrum for a  $\text{LaBr}_3:\text{Ce}$  detector*

Figure 11 shows background data extended to energies above 1750 keV. The presence of low level alpha contaminants is revealed. These have been shown to result from  $^{227}\text{Ac}$  contamination.<sup>10</sup> Detectors produced early in our program contained higher levels of these alpha emitters and subsequent process refinements reduced them to the point that  $^{138}\text{La}$  now produces the dominant background features.<sup>16</sup>

### 38x38 LaBr<sub>3</sub>:Ce and LaBr<sub>3</sub>:Ce,Sr Self Counting



Overall background is summarized in Table 3 for a detector about 38 x38 mm:

Table 3 - Typical Background Count Rates/cc

Background on	LaBr <sub>3</sub> (Ce)	Enhanced LaBr <sub>3</sub> (Ce+Sr)
0-255 keV beta continuum	0,277 Bq/cc	0,272 Bq/cc
790 keV - 1000 keV gamma and beta	0,104 Bq /cc	0,102 Bq/cc
1468 keV gamma peaks	0,063 Bs/cc	0,061 Bq/cc
Alpha above 1600 keV	0,119 Bq/cc* (<0,2 Bq/cc)	0,089 Bq/cc* (<0,2 Bq/cc)

\* These are typical values provided as example. In case of specific need, please contact us.

#### Radiation Hardness

Reports on the relatively good radiation hardness of LaBr:Ce are becoming available<sup>11,12</sup>. These authors conclude that the material is useful for space missions standing up very well to protons and sufficiently to gamma irradiation. Under  $^{60}\text{Co}$  gamma exposure a drop in light output ( -8%) is reported in unpackaged crystals after 1 kGy and the pulse height resolution at 662 keV deteriorates from 3.0% to 3.8%. Thereafter, the authors show the rate of deterioration to slow substantially; and performance is still useful even after exposure to 111 kGy (82% light output, 4.8% FWHM). Recovery with time and temperature is slow and incomplete at best, as their data shows. Related work<sup>13</sup> indicates that details of the packaging are also important to radiation resistance. It's worth remembering that this radiation resistance is much better than that seen with NaI(Tl) or CsI(Tl).

### Mechanically Robust

LaBr<sub>3</sub>:Ce is a robust scintillation crystal at least as rugged as NaI(Tl). Properly packaged detectors of both materials are suitable for systems used in oil well logging behind drill bits, in measurement while drilling operations. These detectors are designed to survive 1000g shock, 30g rms random vibration and 200°C temperatures.

LaBr<sub>3</sub> has an asymmetrical crystal structure and the thermal expansion coefficient is not isotropic. Initially this made crystal yields problematic with boules fracturing while cooling to room temperature. Now Saint-Gobain Crystals has significantly improved the growth process and can grow ingots sufficient to manufacture a 97mm diameter x 244mm long detector. Once the material is grown and cooled to room temperature, it is quite robust.

### TABLE OF SCINTILLATOR PROPERTIES<sup>14</sup> -

Scintillator	Light Yield (photons/keV)	1/e Decay time t(ns)	F.O.M. $\sqrt{t/LY}$	Wavelength of maximum emission $\lambda_m$ (nm)	Refractive index at $\lambda_m$	Density (g/cm <sup>3</sup> )	Thickness (cm) for 50% attenuation (662keV)
NaI(Tl)	38	250	2.6	415	1.85	3.67	2.5
LaBr <sub>3</sub> :Ce	63	16	0.5	380	~1.9	5.08	1.8
LaBr <sub>3</sub> :Ce+Sr	73	25		385	~2.0	5.08	1.8
BaF <sub>2</sub>	1.8	0.7	0.6	~210	1.54	4.88	1.9
LYSO	33	36	1.1	420	1.81	7.1	1.1
BGO	9	300	5.8	480	2.15	7.13	1.0

## FOOTNOTES –

Compiled and Edited by C. M. Rozsa, Peter R. Menge, and M. R. Mayhugh. Originally prepared for distribution by Saint-Gobain Crystals at IEEE NSS/MIC San Diego CA, November 2006.

<sup>1</sup> E.V.D. van Loef , P. Dorenbos, C.W.E van Eijk, H.U. Gudel, K.W. Kraemer, Applied Physics letters, **77**, 1467-1469 (2000).

<sup>2</sup> E.V.D. van Loef , P. Dorenbos, C.W.E van Eijk, H.U. Gudel, K.W. Kraemer, Applied Physics Letters, **79**, 1573-1575 (2001).

<sup>3</sup> Peter R. Menge, G. Gautier, A. Iltis, C. Rozsa, V. Solovyev to be published in Proceedings of 2006 Symposium on Radiation Measurements and Applications, Ann Arbor MI (2006)

<sup>4</sup> A. Iltis , M. R. Mayhugh, P. R. Menge, C. Rozsa, O. Selles, V. Solovyev, III Workshop on Advanced Transition Radiation Detectors Proceedings, Ostuni, Italy Sept 7-10, 2005, to be published in Nucl. Instr. and Meth. A.

<sup>5</sup> C. M. Rozsa, M. R. Mayhugh, P. R. Menge Presentation to the 51st Annual Health Physics Society Meeting, Providence Rhode Island, June 27, 2006. Available on our website. Search Rozsa or Health Physics.

<sup>6</sup> Temperature data for NaI(Tl), CsI(Na), CsI(Tl), Plastic Scintillator (BC438), and BGO are from: “Characteristics of Scintillators for Well Logging to 225 °C” by C.M. Rozsa, et al. prepared for the IEEE Nuclear Science Symposium, San Francisco, October 1989. The PMT is held near room temperature. The full text is available at [www.detectors.saint-gobain.com](http://www.detectors.saint-gobain.com). The temperature response for BrillanCe 380 (LaBr3:Ce) and BrillanCe 350 (LaCl3:Ce) were measured in mid 2005 in high temperature packages, again with the PMT held isothermally near room temperature. To overlay the temperature curves from these two eras, the relative pulse heights for BrillanCe 380 (LaBr3:Ce) and BrillanCe 350 (LaCl3:Ce) were measured by comparing 1” diameter x 1” long crystals in low temperature packages to NaI(Tl) of the same size also in a low temperature package. This result placed the curves at 130% and 75% of NaI(Tl) at room temperature, as shown. As mentioned in the text, later data shows BrillanCe 380 (LaBr3:Ce) to be over 160% of NaI(Tl) at room temperature for more recent data all taken in high temperature Ti-sapphire packages. Other groups report similar room temperature light output, 160% NaI(Tl) or greater.

<sup>7</sup> G. Bizarri, J. T. M. de Haas, P. Dorenbos, and C. W. E. van Eijk, Phys. Stat. Sol. (a) **203**, No. 5, R41- R43 (2006)

<sup>8</sup> For details search High Count Rate or Note 519 for the work by Vladimir Solovyev at [www.detectors.saint-gobain.com](http://www.detectors.saint-gobain.com).

<sup>9</sup> Table of Isotopes, Eighth Edition. Richard B. Firestone, Virginia S. Shirley, Ed. John Wiley & Sons (1996)

<sup>10</sup> T.W. Hossbach, W.R. Kaye, E.A. Lepel, B.S. McDonald, B.D. Milbrath, R.C Runkle, L.E. Smith. Nuclear Instruments and Methods in Physics Research, Section A, 547, 2-3, pp 504-510, August 1, 2005

<sup>11</sup> Gamma-Ray Induced Radiation Damage in LaBr3:5%Ce and LaCl3:10%Ce Scintillators. W. Drozdowski, P. Dorenbos, A. J. J. Bos, S. Kraft, E. J. Buis, E. Maddox, A. Owens, F. G. A. Quarati, C. Dathy, and V. Ouspenski, IEEE Transactions on Nuclear Science, Vol. 54, No. 4, August 2007, 1387

<sup>12</sup> Effect of Proton Dose, Crystal Size, and Cerium Concentration on Scintillation Yield and Energy Resolution of LaBr3 :Ce W. Drozdowski, P. Dorenbos, A. J. J. Bos, J. T. M. de Haas, S. Kraft, E. Maddox, A. Owens, F. G. A. Quarati, C. Dathy, and V. Ouspenski IEEE Transactions on Nuclear Science, Vol. 54, No. 3, June 2007

<sup>13</sup> Gamma Ray Induced Radiation Damage in Ø1” × 1” LaBr3:5%Ce Winicjusz Drozdowski, Pieter Dorenbos, Adrie J.J. Bos, Alan Owens, Francesco, G.A. Quarati (Private communication via preprint)

<sup>14</sup> The 2007 version reflects revised density and attenuation coefficients for the BrillanCe materials.

<sup>15</sup> The 2009 version reflects new temperature response data.

<sup>16</sup> The 2021 version reflects new background data.